Experimental and thermal study of a designed linear solar receiver without metal tube

Djelloul Azzouzi[1, 2,*], Adel Lakhdar Ezzine[1] , Mohamed Doucha Dhiaeddine[1]

[1]Faculty of sciences and technology, University of Khemis Miliana, Algeria

[2]Industrial fluids laboratory, measurements and applications, University of Khemis Miliana, Algeria

*corresponding Author: Road of Tissemsilt, University of Khemis Miliana, Algeria. Email: azzouzidjelloul@yahoo.fr , Phone +213773455352

Abstract

Thermal efficiency improvement of the concentrated solar power plants is closely related to the thermal performance of their solar receivers placed along the focal zone of the parabolic trough concentrators. In this paper, an experimental and thermal analysis of a linear solar receiver without metal tube is presented. The solar receiver composed of two coaxial glass pipes between them a vacuum annular volume has been realized. Then, the designed receiver is placed at the focal zone of PTC in order to investigate its thermal efficiency. It should be noted that water is used as HTF circulating into the solar receiver. The wind speed effect was not taken into account in experimental process carried out under a receiver inclination angle of 36° corresponding to the experimentation site latitude. It is found that, the maximum thermal efficiency of the receiver records a value of 49%. Thermal analysis of the receiver through the developed thermal model written in Matlab software takes into considerations all heat transfer modes. Experimental results and those obtained analytically remain in acceptable adequacy.

Keywords: parabolic trough, solar receiver, heat loss, thermal efficiency.

1. Introduction

Parabolic trough solar collectors are largely used as basic elements in a great number of concentrated solar power plants realized during the last decade [1]. Benefits of using PTC technology are justified by a moderate investment cost as well as its ease of coupling with other energy sources [2]. Their mode of linear solar concentration requires that, the exploited linear receivers must have an acceptable thermal efficiency in order to ensure a maximum conversion of the available focused solar flux in focal zone [3]. It is useful to note that, the thermal characteristics of the heat transfer fluid circulating in the solar receiver affect appreciably its thermal efficiency [4,5] and limit the operating temperature level of the solar thermal power plant [6,7]. Numerous studies have been focused on the thermal efficiency improvement of the solar linear receivers through the investigation of a new geometrical designs and the use of nanofluids as HTFs. Wang et al [8] present a numerical study of a PTC using a tube receiver by inserting with metal foams. Results show that the thermal efficiency of the tube receiver with metal foams inserts was increased from 10 to 50% compared to the conventional tube receiver. In order to improve the thermal efficiency, an experimental investigation of porous disc enhanced tube receiver was carried out by Reddy et al [9]. A numerical study of the thermal performance of a linear receiver with perforated plate insert was presented by Agrrey et al [10]. Analyses indicated that the thermal efficiency increased up to 8%. In the aim of increasing the overall heat transfer performance, numerous type of linear receiver has been developed. Huang et al [11] introduced a numerical study of a dimpled tube used as metal tube of tube receiver. They found an increase of the heat exchange surface inducing a growth in the collector thermal efficiency. A compound copper-steel tube receiver was developed by Flores and Almanza [12] for the solar power plant of the National university of Mexico. Bellos et al [13] examined the thermal enhancement through the use of a converging-diverging receiver tube. Results indicate that the thermal efficiency recorded an increase of about 4.55% compared to the conventional tube receiver. In this paper, an

experimental and thermal analysis of a designed solar receiver is presented. The first stage is devoted to the design steps and geometrical description of the designed receiver followed by an experimental investigation in order to determine the HTF outlet temperature and its thermal efficiency. A developed thermal model is presented in a second stage in which, all existing heat exchange between the various receiver elements were considered.

2. Materials and methods

2.1. Description of the designed receiver

The linear receiver used in this current study as indicated in Fig. 1 is composed of two glass coaxial tubes having a length of 160 cm. The glass cover which represents the external tube has respectively an internal and external diameter of 20 mm and 24 mm, while the interior tube (absorber) has an inner diameter of 8mm with a thickness of 1.5mm.

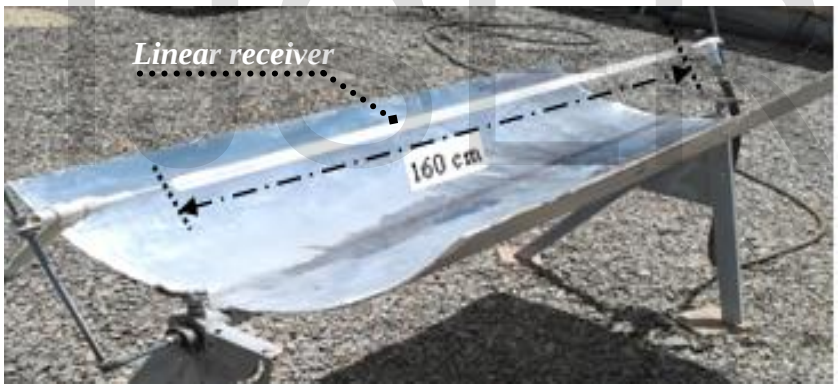

Fig. 1. Front view of the designed linear receiver assembled to the parabolic trough concentrator.

Thermophysical proprieties of the used glass are indicated in table 1. The annular volume located between the two tubes has a volume of 1.402 dm^3. It should be noted that the value of the external cover glass diameter was defined after the determination of the focused sunspot width of the parabolic trough concentrator used in experiment.

Table 1. Physical proprieties of the used glass

Thermal conductivity (W/m.K)	1.04
Density (kg/m^3)	3214

Specific heat (kJ/kg.°C)	0.72
Melting point (°C)	1380
Emissivity	0.92

2. Experimental procedure

The experimental tests were carried out in the solar experimentation site located at Khemis Miliana University (Algeria). The first step is devoted to the positioning of the solar receiver at the focal zone of the parabolic trough concentrator. In table 2 are indicated the geometrical and optical properties of the used concentrator. It should be noted that the solar receiver is placed at 1.2 cm below the real focal length in order to ensure a uniform distribution of the focused solar flux along its glass cover as schematized in Fig. 2 by using the Soltrace software.

Table 2. Parabolic trough concentrator parameters

Aperture area	1.184 m^2
Reflecting surface	1.44 m^2
Concentrator depth	23cm
Theoretical focal length	14.88 cm
Rim angle	106°
Concentrator reflectivity	0.86
Tracking mechanism	mechanical

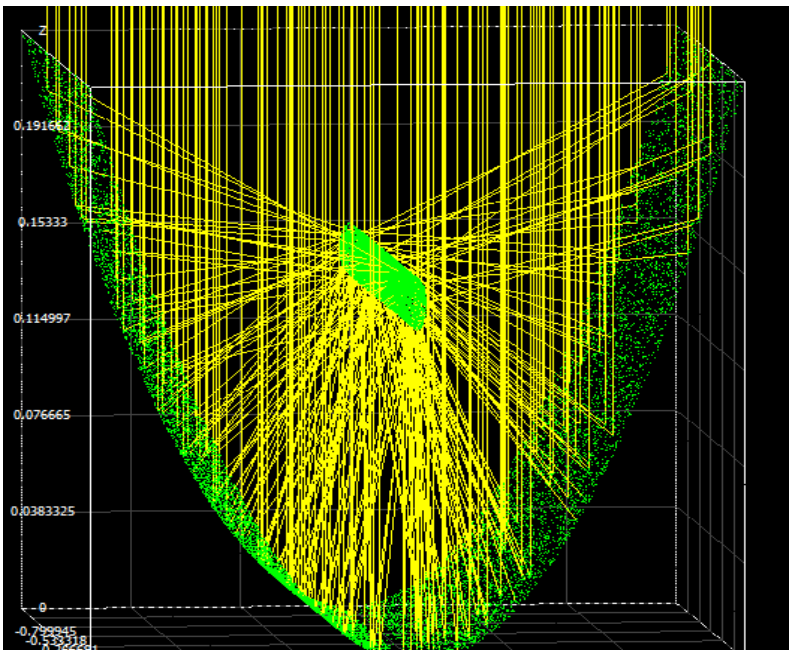

The experimental set-up as consists of a 0.736 kW centrifugal pump ensuring the working fluid circulation through the solar receiver. The working fluid (water) circulating in receiver is supplied from a water tank of 200 L capacity while the water mass flow rate is controlled by a needle valve and measured by a flowmeter. The inlet and exit water temperatures are measured using k- thermocouples which are connected to a data acquisition. It should be noted that the system operates in closed cycle and the wind speed effect is not taken into account. The thermocouples uncertainty is about 0.5 % for measurements between 20 °C and 175 °C, while the flowmeter has an uncertainty of about ± 0.4 % for 1.5 l/min measurement. The direct normal insolation was measured during the experiments by, the CMP11 pyranometer. Two experimental tests were carried out to determine respectively; the time-constant and the receiver thermal efficiency. In the first test which consists to evaluate the time constant defined by the necessary duration so that the thermal steady state is established, water near ambient temperature of about 27 °C is circulated at 0.6 l/min after the focusing of the parabolic trough concentrator. Once the steady state conditions are reached the concentrator is then defocused and the time constant value is determined for each water flow rate. The second experimental part is devoted to the determination of the absorber thermal efficiency during which, the water flow rate pumped was varied from 0.5 l/min to 6 l/min.

3. Analytical development

The linear solar receiver scheme as represented in Fig. 3a is thermally analysed in order to determine its thermal efficiency defined as, the report between the useful heat flux

Q_{htf} absorbed by the heat transfer fluid (HTF) circulating inside glass pipe and solar flux focused Q_{Foc} uniformly along the glass cover external surface as illustrated in Fig. 3b. This efficiency can be determined through the energy balance involving the various heat flux and heat losses in each section of the solar receiver. So, the evaluation of the thermal losses evacuated through the different heat transfer modes is considered as a significant factor in the optimization of the designed receiver.

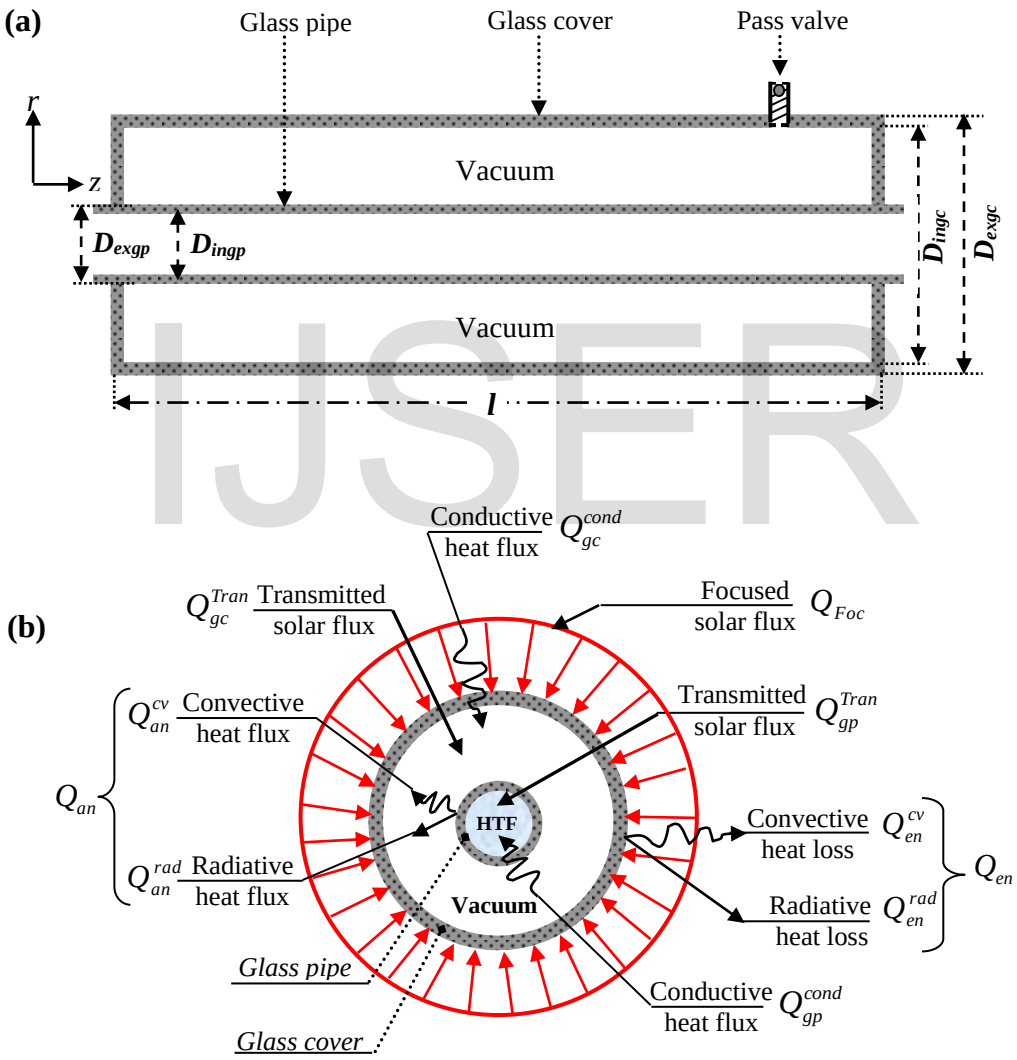

Fig. 3. Descriptive scheme of the linear solar receiver (a) dimensional representation, (b) heat transfer nomenclature.

3.1. External heat loss

The heat transfer from the glass cover to the surrounding occurs by convection and radiation. In this application where radiation is combined with other modes of heat transfer, the solution can often be simplified by using the different thermal resistances of each heat transfer. The external heat loss Q_{en} is expressed by the following relation:

$$Q_{en} = \frac{T_{exgc} - T_{amb}}{R_{en}} \tag{1}$$

Here $T_{exgc} - T_{amb}$ is the temperature gradient between the external glass cover and that of ambient air as indicated in Fig. 4b. R_{en} is the environment thermal resistance given as follows:

$$R_{en} = \frac{1}{h_{en} A_{exgc}} \tag{2}$$

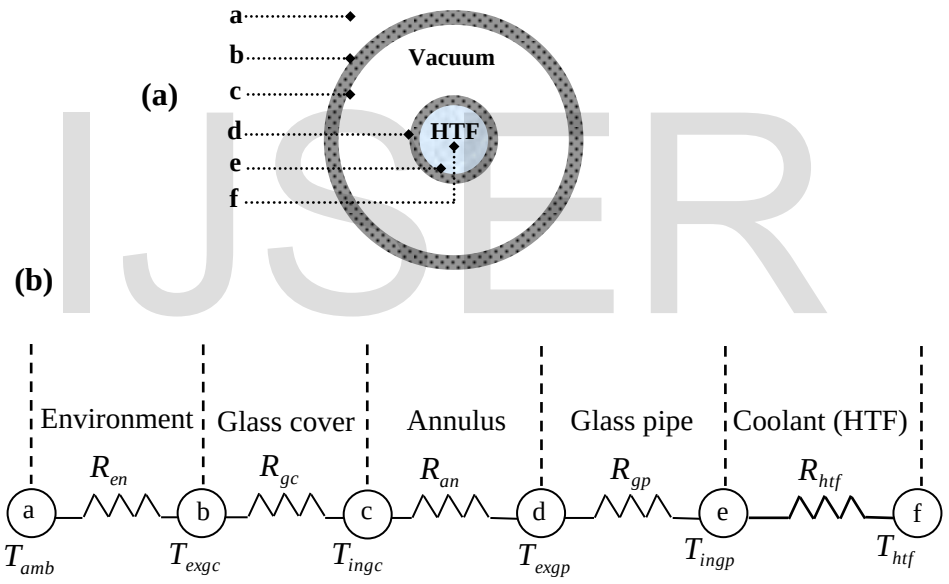

Fig. 4. Receiver radial surface (a) cross section nomenclature, (b) thermal resistances model.

In Eq. (2) appear the external glass cover surface A_{exgc} and the external heat transfer coefficient h_{en} given by the following expression:

$$h_{en} = h_{en}^{cv} + h_{en}^{rad} \tag{3}$$

The convective heat transfer coefficient of external environment h_{en}^{cv} is determined as follows:

$$h_{en}^{cv} = \frac{Nu\, K_{air}}{D_{exgc}} \tag{4}$$

Where the Nusselt number Nu developed by Churchill and Chu [14] is given by Eq. (5) in which all thermo-physical proprieties are calculated at the average temperature $\left(T_{amb}+T_{exgc}\right)/2$.

$$Nu=\left[0.60+\frac{0.387Ra^{1/6}}{\left(1+\left(0.559/Pr_{air}\right)^{9/16}\right)^{8/27}}\right]^2 \tag{5}$$

It should be noted that the Nusselt number as formulated in Eq. (5) is applied when there is no wind and heat transfer occurs by natural convection from glass cover to ambient air. The Rayleigh number, thermal expansion coefficient and Prandt number are expressed respectively by the Eqs. (6), (7) and (8).

$$Ra=\frac{g\beta\left(T_{exgc}-T_{amb}\right)D_{exgc}^3}{\upsilon_{air}^2}Pr_{air} \tag{6}$$

$$\beta=\frac{1}{T_{amb}} \tag{7}$$

$$Pr_{air}=\frac{\mu_{air}\left(C_p\right)_{air}}{K_{air}} \tag{8}$$

Radiation heat transfer coefficient of external environment h_{en}^{ra} can be determined through the Stephan-Boltzmann law given as follows:

$$Q_{en}^{rad}=\sigma\varepsilon_{exgc}A_{exgc}\left(T_{exgc}^4-T_{sky}^4\right)=h_{en}^{ra}A_{exgc}\left(T_{exgc}-T_{sky}\right) \tag{9}$$

from where:

$$h_{en}^{rad}=\frac{\sigma\varepsilon_{gc}\left(T_{exgc}^4-T_{sky}^4\right)}{T_{exgc}-T_{sky}} \tag{10}$$

Where T_{sky} is the sky temperature determined by the following expression [22]:

$$T_{sky}=0.0552T_{amb}^{1.5} \tag{11}$$

The Stephan-Boltzmann constant σ is equal to $5.6\times10^{-8}W.m^{-2}.K^{-4}$ and ε_{exgc} is the emittance of the external glass cover surface [16].

Note that h_{en}^{rad} depends strongly on temperature, while the temperature dependence of the convection heat transfer coefficient h_{en}^{cv} is generally weak [15].

3.2. Heat transfer through the glass cover

As shown in Fig. 4 and Fig. 3b, the thermal resistance R_{gc} of the glass cover is crossed by the transmitted solar flux Q_{gc}^{Tran} and the heat flux Q_{gc}^{cond} transferred by conduction through the glass cover wall (semitransparent material). The thermal balance in this section can be written as follows:

$$Q_{Foc} - Q_{en} = Q_{gc}^{Tran} + Q_{gc}^{cond} \tag{12}$$

Where:

$$Q_{Foc} = \bar{\rho} E_s C A_{exgc} \tag{13}$$

$$Q_{gc}^{Tran} = \alpha \ Q_{Foc} \tag{14}$$

$$Q_{gc}^{cond} = \frac{T_{exgc} - T_{ingc}}{R_{gc}} \tag{15}$$

$$R_{gc} = \frac{ln\left(D_{exgc} \big/ D_{ingc}\right)}{2\pi K_{gc} L} \tag{16}$$

In Eq. (14) appears α as the transitivity factor which takes a same value for the glass cover and the glass pipe.

3.3. Heat exchange in annular space

In this receiver space (enclosure) located between external glass pipe and internal glass cover; heat transfer occurs by convection and radiation expressed as follows:

$$Q_{an} = Q_{an}^{cv} + Q_{an}^{rad} = \frac{T_{ingc} - T_{exgp}}{R_{an}} \tag{17}$$

Where Q_{an}^{cv} and Q_{an}^{rad} are respectively the convective and radiative heat fluxes at the annular space and R_{an} is the annulus thermal resistance determined by the following expression:

$$R_{an} = \frac{1}{2\pi h_{an} L} \tag{18}$$

The annulus heat transfer coefficient h_{an} as indicated in Eq. (18) is evaluated under vacuum condition. In this annular space (enclosure) located between external glass pipe and internal glass cover; heat transfer occurs by convection and radiation. It should be noted that the convection heat transfer at pressure lower than 0.013 Pa [17] occurs by free molecular convection.

$$h_{an} = h_{an}^{cv} + h_{an}^{rad} \tag{19}$$

Where the annulus convective heat transfer h_{an}^{cv} is given by [18]:

$$h_{an}^{cv} = \frac{K_{std}}{\dfrac{D_{exgp}}{2\,ln\left(\dfrac{D_{ingc}}{D_{exgp}}\right)} + b\lambda\left(\dfrac{D_{exgp}}{D_{ingc}} + 1\right)} \tag{20}$$

For a Rayleigh number $Ra_{D_{ingc}} < \left(\dfrac{D_{ingc}}{D_{ingc} - D_{exgp}}\right)^4$

In Eq. (20) appear the thermal conductivity K_{std} of annulus gas at standard condition and the interaction coefficient b which take respectively a values of 0.02551W/m.°C and 1.571, while the specific heats ratio for the annulus gas λ is equal to 1.31 [19].

The radiative heat transfer coefficient h_{an}^{ra} is evaluated by the following expression [21]:

$$h_{an}^{rad} = \frac{\sigma\left(T_{exgp}^4 - T_{ingc}^4\right)}{\left(\dfrac{1}{\varepsilon_{exgp}} + \left(\dfrac{\left(1-\varepsilon_{ingc}\right)D_{exgp}}{\varepsilon_{ingc} D_{ingc}}\right)\right)\left(T_{exgp} - T_{ingc}\right)} \tag{21}$$

3.4. Heat transfer through the glass pipe

The thermal resistance R_{gp} of the glass pipe is crossed by the transmitted solar flux Q_{gp}^{Tran} and the heat flux Q_{gp}^{cond} transferred by conduction through the glass pipe wall. In this section, heat exchange can be characterized by the following heat balance:

$$Q_{gc}^{Tran} + Q_{gc}^{cond} - Q_{an} = Q_{gp}^{cond} + Q_{gp}^{Tran} \tag{22}$$

Where:

$$Q_{gp}^{Tran} = \alpha Q_{gc}^{Tran} = \alpha^2 Q_{Foc} \tag{23}$$

$$Q_{gp}^{cond} = \frac{T_{exgp} - T_{ingp}}{R_{gp}} \tag{24}$$

$$R_{gp} = \frac{ln\left(D_{exgp} \big/ D_{ingp}\right)}{2\pi K_{gp} L} \tag{25}$$

3.5. Heat transfer from glass pipe to heat transfer fluid

At the steady state, the heat balance is expressed as follows:

$$Q_{gp}^{cond} + Q_{gp}^{Tran} = Q_{htf} \tag{26}$$

Where Q_{htf} is the useful heat flux absorbed by the heat transfer fluid circulating inside glass pipe. The absorbed flux is given by the following expression:

$$Q_{htf} = \frac{T_{ingp} - T_{htf}}{R_{htf}} \tag{27}$$

Where R_{htf} is the thermal resistance of the heat transfer fluid given as follows:

$$R_{htf} = \frac{1}{\pi D_{ingp} L\ h_{htf}} \tag{28}$$

The useful heat transfer coefficient h_{htf} as indicated in Eq. (28) is determined by Eq. (29).

$$h_{htf} = \frac{Nu_{htf}\ K_{htf}}{D_{ingp}} \tag{29}$$

Where Nu_{htf} is the Nusselt number of the heat transfer fluid which strongly depends on the type of flow through the glass pipe [25]. In the case of laminar- flow when Reynolds number is lower than 2300, Hall et al [21] shows that the Nusselt number is a function only of the type of heating boundary condition and, for a boundary condition with a constant heat flux, Nusselt number takes a constant value of 4.364. For transitional and turbulent cases which occur at Reynolds number greater than 2300, Gnielinski [23] proposed a modified correlation of that suggested by Petukhov [24] to extend its applicability in this Reynolds number range in order to determine the Nusselt number as follows:

$$Nu_{htf} = \frac{(Re-1000)Pr\,(f/2)}{1+12.7\left(Pr^{2/3}-1\right)\sqrt{f/2}}\left(\frac{Pr}{Pr_w}\right)^{0.11} \tag{29}$$

Where the friction coefficient f is determined through the Eq. (31)

$$f = (1.58\,ln\,Re - 3.28)^{-2} \tag{31}$$

3.6. Receiver thermal efficiency

The receiver thermal efficiency is defined as the report/ratio between the heat flux Q_{htf} absorbed by the heat transfer fluid circulating inside glass pipe and the solar flux Q_{Foc} focused at the outside glass cover. It is expressed analytically as:

$$\eta = \frac{Q_{htf}}{Q_{Foc}} \tag{32}$$

The outlet temperature of the heat transfer fluid can be obtained through the Eq. (33) given as follows:

$$T_{out} = T_{in} + \frac{Q_{htf}}{\dot{m}_{htf}\,(C_P)_{htf}} \tag{33}$$

Where the mass flow rate $\dot{m}_{htf}$ of the heat transfer fluid is given by:

$$\dot{m}_{htf} = (1/60)\,\rho_{htf}\dot{V}_{htf} \tag{34}$$

The coefficient (1/60) which appears in Eq. (34) corresponds to the conversion unit from min^{-1} to s^{-1}.

4. Results and discussion

Through the Fig. 5 which presents the measured temperatures at various receiver positions under a direct normal insolation (DNI) of 560 W/m², it appears that the temperature increases up to its maximum of about 132.3°C reached at a distance of 15 cm. This distance indicates exactly to the real focal length of the parabolic trough concentrator. The insignificant difference of 1mm between the theoretical focal length as indicated in Table 2 and that determined in experiment explains the good adherence obtained during joining operation.

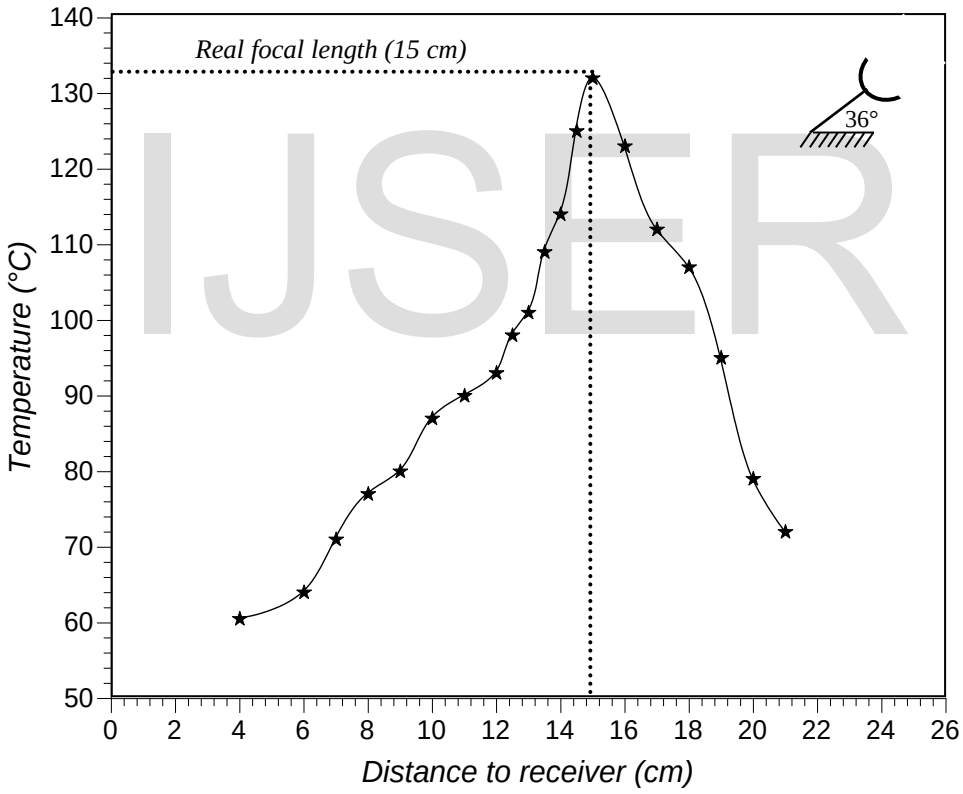

Fig. 5. Measured temperature at various receiver positions along the focal axis.

Fig. 6 shows the radial temperature distribution along the surface receiver which allows the determination of the sunspot width size. It should be noted that this experiment process is carried out under a solar irradiation of 680 W/m². It appears that the maximal temperature is reached exactly at the focal line recording a value of about 164°C. The sunspot width is delimited between the two isothermal of 60°C which indicates a size of 23 mm giving a

sunspot surface of 368 cm². The knowledge of the sunspot surface leads us to determine the real concentration ratio and the focused solar flux which take respectively a value of 31.83 and 21.64kW/m².

It can be seen through the Fig. 7, the three distinct zones which figure in the water outlet temperature variation with time. The first one is located between 0 and 1min in which an insignificant temperature variation is recorded. This observation can be explained by the weak capacitive effect of glass cover on heat exchange within the solar receiver during this short period.

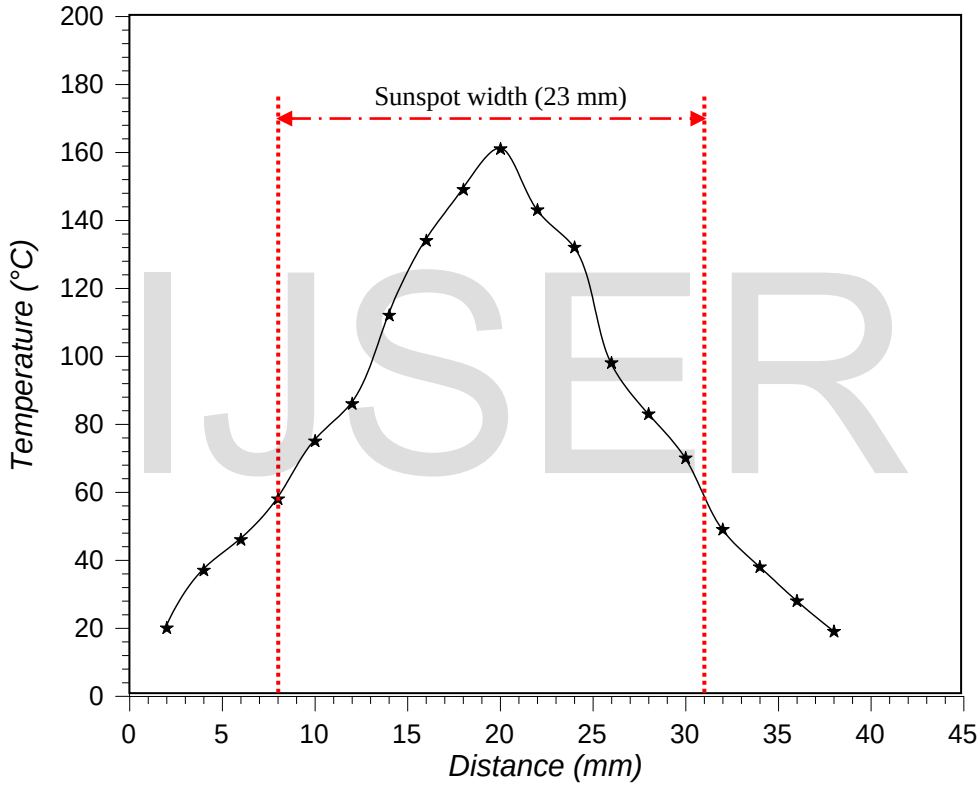

Fig. 6. Measured temperature along the width of the plate receiver positioned at a PTC focal zone.

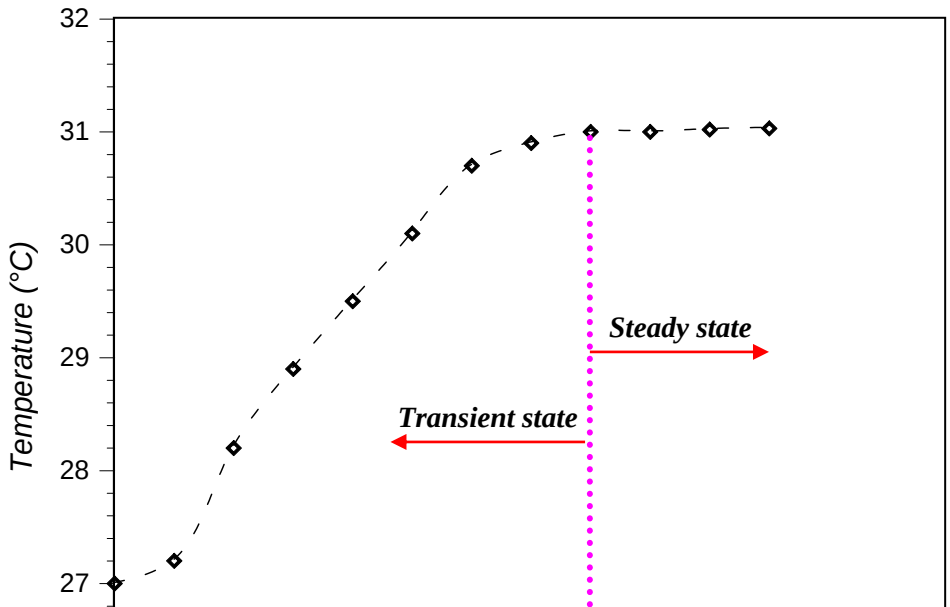

The second zone ranging between 1 to 8 min is characterised by a significant increase of the water outlet temperature which passes from a value of 27.2°C to 31°C. The two preceding zones are located in the transient state interval. Beyond 8 min, no variation in water outlet temperature is recorded what indicates that the steady state is established. It should be noted that the value of 8 min represents the time constant of the solar receiver.

Fig. 8 represents the experimental and analytical results of $(T_{out} - T_{in})$ according to the water flow rate circulating in the solar receiver under a direct normal insolation of 620 *W/m²*. It is noted that $(T_{out} - T_{in})$ is appreciably affected by the water flow rate variation. it appears that the rise of the flow rate from 0.5 to 3 l/min causes a reduction in $(T_{out} - T_{in})$ from 3.9 to 0.6°C recording a rate about 1.32°C/(l/min) , while the analytical variation records a diminution from 4.7 to 1.4°C which corresponds to the same rate recorded in experiment.

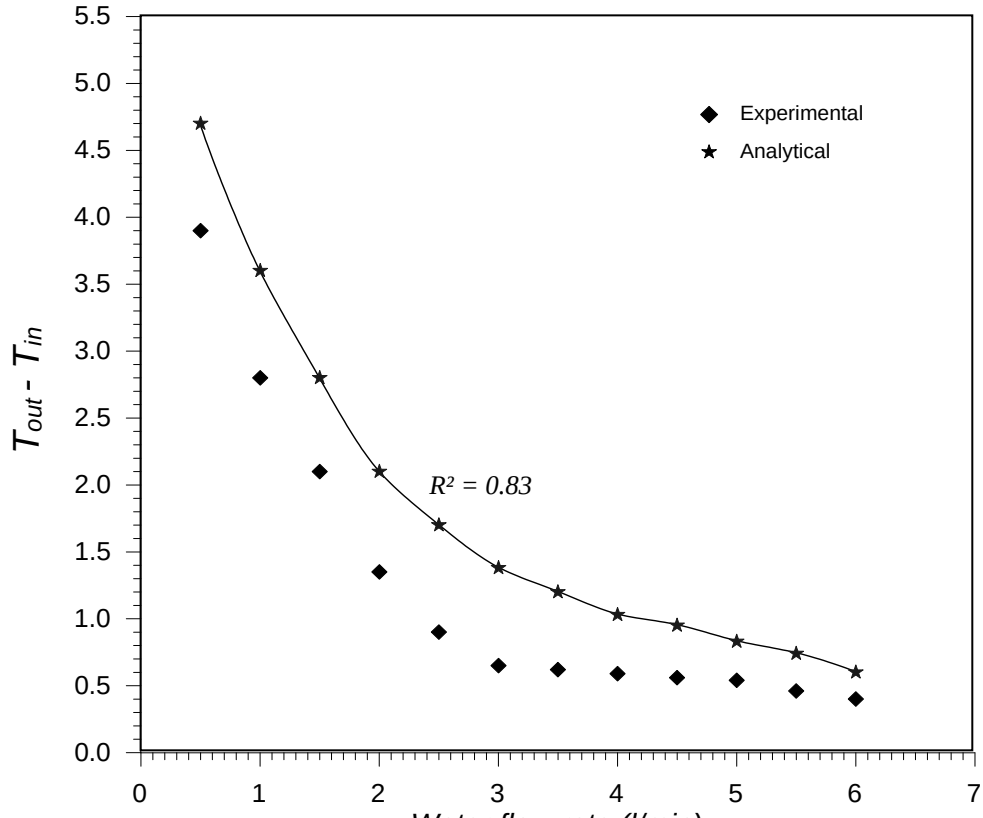

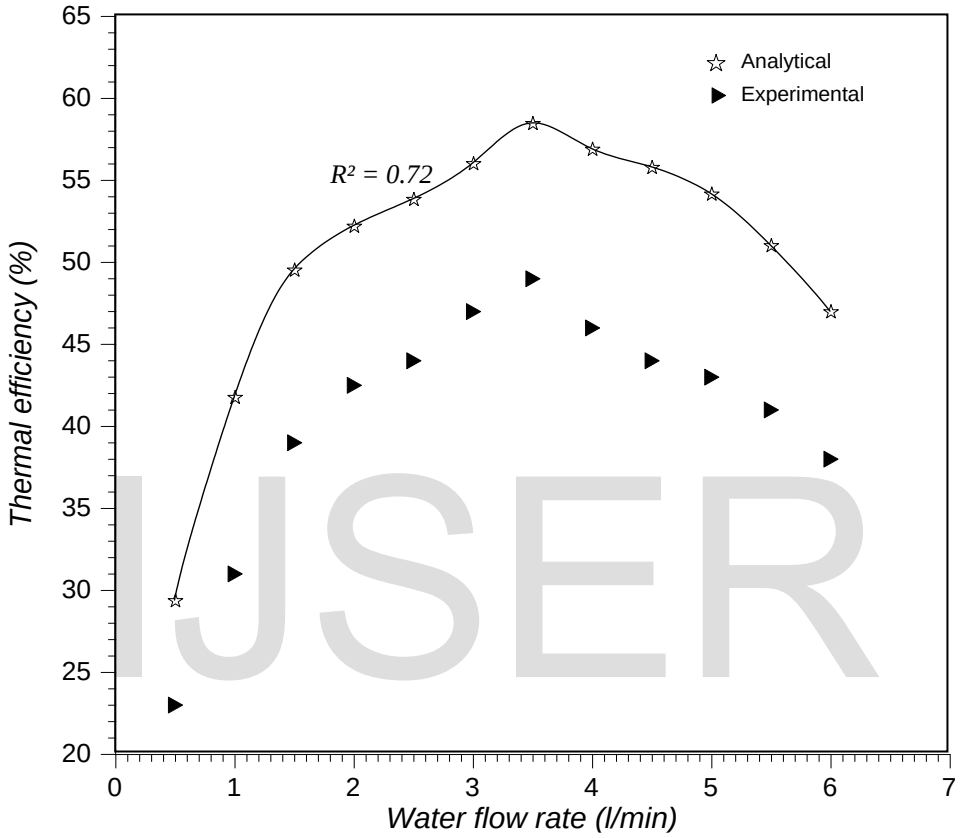

Fig. 9. Experimental and analytical variation of the thermal efficiency with water flow rate under solar irradiation $E_s = 620\ W/m^2$.

Fig. 9 shows that the thermal efficiency calculated experimentally and analytically varies with water flow rate differently in two distinct zones. The first one is that ranging between 0.5 to 3.5 l/min in which the thermal efficiency increases to its maximum experimental value of about 49% recorded at 3.5 l/min. The second zone is represented in the interval going from 3.5 to 6 l/min in which the thermal efficiency decreases with the increase of the water flow. This decrease in thermal efficiency is affected by the reduction of the useful heat transfer coefficient h_{htf} due to the strong increase in turbulence of the water flow. It appears that the

analytical results of the thermal efficiency take the same pace as experimental with a standard error of about 0.72.

5. Conclusion

In this paper, the designed linear receiver placed at the focal zone of the parabolic trough concentrator with large rim angle was studied in experiments and analytically. It should be noted that the focal length of the used PTC calculated in experiments remain in good adequacy with that determined analytically. It was found that the thermal efficiency of the linear receiver is appreciably affected by the flow rate variation of the heat thermal fluid circulating in its internal glass pipe. Based on the developed analytical thermal model, the evaluation of outlet temperature and thermal efficiency of the solar linear receiver can be predicted with an acceptable precision.

Acknowledgements

This work was supported by the laboratory of Industrial fluids, measurements and applications of Khemis Miliana University.

References

[1] Md. Tasbirul Islam, Nazmul Huda, A.B. Abdullah , R. Saidur, 2018. A comprehensive review of state-of-the-art concentrating solar power (CSP) technologies: Current status and research trends. Renewable and Sustainable Energy Reviews 91, 987–1018.

[2] F. Wang, Z. Cheng, J. Tan, Y. Yuan, Y. Shuai, L. Liu, 2017. Progress in concentrated solar power technology with parabolic trough collector system: A comprehensive review. Renewable and Sustainable Energy Reviews 79, 1314-1328.

[3] D. Azzouzi , H.E. Bourorga, K.A. Belainine, 2018. Experimental study of a designed solar parabolic trough with large rim angle. Renewable Energy 125, 495-500.

[4] H.M, Sandeep, U.C. Arunachala, 2017. Solar parabolic trough collectors: a review on heat transfer augmentation techniques. Renew Sustain Energy 69, 1218-1231.

[5] K. Alibakhsh, TE. Amin, S. Mohammad 2015. A review on the applications of nanofluids in solar energy systems. Renew Sustain Energy Rev 43, 584-598.

[6] M. Ouagued, A. Khellaf, L. Loukarfi, 2013. Estimation of the temperature, heat gain and heat loss by solar parabolic trough collector under Algerian climate using different thermal oils. Energy Convers Manage 75,191-201.

[7] O. Mahian, A. Kianifar, S.A. Kalogirou, I. Pop, S. Wongwises, 2013. A review of the applications of nanofluids in solar energy, International Journal of Heat and Mass Transfer 57, 582-594.

[8] P. Wang, DY. Liu, C. Xu, 2013. Numerical study of heat transfer enhancement in the receiver tube of direct steam generation with parabolic trough by inserting metal foams. Appl Energy 102, 449-60.

[9] KS. Reddy, KK. Ravi, CS. Ajay, 2015. Experimental investigation of porous disc enhanced receiver for solar parabolic trough collector. Renew Energy 77, 308-19.

[10] M. Aggrey, BO. Tunde, PM. Josua, 2014. Heat transfer and thermodynamic performance of a parabolic trough receiver with centrally placed perforated plate inserts. Appl Energy 136, 989-1003.

[11] Z. Huang, ZL. Li, GL. Yu, WQ. Tao, 2017. Numerical investigations on fully–developed mixed turbulent convection in dimpled parabolic trough receiver tubes. Appl Therm Eng 114, 1287-1299.

[12] VC. Flores, RF. Almanza, 2004. Behavior of compound wall copper–steel receiver with stratified two–phase flow regimen in transient states when solar irradiance is arriving on one side of receiver. Solar Energy 76, 195-208.

[13] E. Bellos, C. Tzivanidis, K.A. Antonopoulos, G. Gkinis., 2016. Thermal enhancement of solar parabolic trough collectors by using nanofluids and converging–diverging absorber tube. Renew Energy 94, 213-222.

[14] S.W. Churchill and H.H.S. Chu, 1975. Correlating Equations for Laminar and Turbulent Free Convection from a Horizontal Cylinder. International Journal of Heat and Mass Transfer18, 1049-1053.

[15] F.Kreith and W. Z. Black, Basic Heat Transfer, Harper and Row, New York, 1980.

[16] YS. Touloukian. Radiative properties, nonmetalic solids, thermophysical properties of matter, vol. 8. New York: Plenum Publishing,1972.

[17] KJC Operating Company. Final report on HCE heat transfer analysis code, SANDIA Contract No. AB-0227; 1993.

[18] A. Ratzel, C. Hickox, D. Gartling, 1979. Techniques for reducing thermal conduction and natural convection heat losses in annular receiver geometries. Journal of Heat Transfer 101,108-113.

[19] Marshal N. Gas Encyclopedia. New York: Elsevier; 1976.

[20] Cengel YA. Heat transfer and mass transfer: a practical approach. 3rd ed. McGraw Hill Book Company; 2006.

[21] W.B. Hall, J.D. Jackson, P.H. price, 1963,Note on forced convection in a pipe having heat flux which varies exponentially along its length, J.Mech.Eng.Sci., Vol.5, pp. 40-52.

[22] O. Garcia-Valladares and N. Velazquez, 2009. Numerical simulation of parabolic trough collector: improvement using counter flow concentric circular heat exchangers. Int J Heat Mass Transf 52, 597-609.

[23] V. Gnielnski, 1976. New equations for heat and mass transfer in turbulent pipe and channel flow. International Chemical Engineering 562, 359-368.

[24] B.S. Petukhov, heat transfer and friction in turbulent pipe flow with variable physical proprieties. Advances in heat transfer, ed. J.P. Irvine and T.F. Hartnett, Vol. 6, pp. 503-564, Academic, New York, 1970.

[25] S.A. Kalogirou, 2012. A detailed thermal model of a parabolic trough collector receiver. Energy 48, 298-306.

Nomenclature

A : area (m^2)

C : solar concentration ratio

C_p : specific heat of air $\left(J/kg.K\right)$

D : diameter (m)

E_s : solar irradiation (W/m^2)

e : thickness (m)

f : friction coefficient

Gr : Grashof number

g : acceleration of gravity (m/s^2)

h : heat transfer coefficient $\left(W/m^2.K\right)$

K : thermal conductivity $\left(W/m\ .K\right)$

L : length (m)

$\dot{m}$: mass flow rate $\left(kg/s\right)$

Nu : Nusselt number

Pr : Prandtl number

Q : heat flux (W)

R : thermal resistance (K/W)

Ra : Rayleigh number

Re : Reynolds number

T : temperature (K)

$\dot{V}$: volumetric flow rate (l/min)

Subscripts

air: air

amb: ambient

an : annulus

cond: conduction

cv: convection

en: environment

exgc: external glass cover

Foc: focused

gc: glass cover

gp: glass pipe

htf: heat thermal fluid

in: inlet

ingc: internal glass cover

out: outlet

rad: radiation

sky: sky

Trans: transmitted

w: wall

Greek symbols

α : reflectivity factor

β : coefficient of thermal expansion $\left(K^{-1}\right)$

ε : emissivity

μ : dynamic viscosity $\left(kg/m.s\right)$

υ : kinematic viscosity $\left(m^2/s\right)$

η : thermal efficiency

ρ : density $\left(kg/l\right)$

$\overline{\rho}$: concentrator trough reflectivity

σ : stefan-Boltzman constant $(W m^{-2} K^{-4})$